Macromolecules
ARTICLE

*Macromolecules* **2010**, *43*, 10659–10667 **10659**
DOI: 10.1021/ma102055w

# Simulations of Dendrimers with Flexible Spacer Chains and Explicit Counterions under Low and Neutral pH Conditions

**J. S. Kłos*,†,§ and J.-U. Sommer†,‡**

†*Leibniz Institute of Polymer Research Dresden e. V., 01069 Dresden, Germany,* ‡*Institute for Theoretical Physics, Technische Universität Dresden, 01069 Dresden, Germany, and* §*Faculty of Physics, A. Mickiewicz University, Umultowska 85, 61-614 Poznań, Poland*

*Received September 4, 2010; Revised Manuscript Received October 28, 2010*

ABSTRACT: We study the properties of weak dendritic polyelectrolytes of generation $G = 5$ with flexible spacers of various lengths and explicit counterions in an athermal solvent using Monte Carlo simulations based on the bond fluctuation model. The calculations are performed for molecules under neutral and low pH conditions. At neutral pH we assume that only the terminal groups of the dendrimers bear positive charges, while at low pH both the terminal groups and the branching units are charged. In our study, the full Coulomb potential and the excluded volume interactions are taken into account explicitly with the reduced temperature $\tau$ as the main simulation parameter. We observe an interplay of condensation of counterions, trapping of counterions inside the dendrimer's volume and evaporation of counterions into the surrounding solution giving rise to a nonmonotonous electrostatic swelling of the dendrimer with temperature. Decreasing pH leads to higher swelling and stronger spacer-length dependence. At low pH spacer length-scaling cannot be applied and longer spacers shift the maximum of the swelling to lower temperature. To explain the swelling effect we apply a Flory-type argument where both trapped but noncondensed counterions and uncompensated charges due to evaporation of counterions are taken into account. This model properly reflects the swelling behavior with respect to temperature, pH and spacer-length variation, but quantitatively underestimates the swelling effect. We further investigate the pH-effects on density and charge profiles of the dendrimer.

## I. Introduction

Dendrimers are chemically synthesized molecules whose properties are nowadays studied most intensively. These molecules consist of subsequent generations of linear chains (called spacers) arranged in a hierarchical, treelike structure. Starting with the central core as the initiator they can be made iteratively generation by generation by attaching new spacers to the two-functional ends (branching points) of the outermost, terminal chains.

The interest in dendrimers is mainly based on their potential applications in various fields ranging from materials engineering to biomedicine and pharmacy. To name but a few, dendrimers have been used to deliver oligonucleotides to the cell.[1,2] They enhance cytosolic and nuclear availability as indicated by confocal microscopy as well as cell uptake and transfection efficiency of plasmid DNA.[3] Guest−host nanodevices such as gold/PAMAM (polyamidoamine dendrimers) nanocomposites are potentially very useful agents for improving the imaging and radiation treatment of cancer.[4]

Of a particularly increasing interest of both theoretical and experimental research are properties of weak dendritic polyelectrolytes. These molecules are not fully charged in solution, and their charge can be modulated by changing the solution pH. For instance, PAMAM and poly(propyleneimine) dendrimers acquire positive charge because they have primary amine groups at the terminal units and tertiary amine groups at the branching points which become protonated as the solution pH-value is lowered from around 7 down to 4, respectively.[5−10] In other words, in physiological conditions only the terminal groups of PAMAMs bear positive charges, whereas in more acidic environments both the terminal groups and branching groups do.

*Corresponding author.

Whether or not the above charge modulation has a pronounced effect on conformational and structural properties of charged dendrimers has been the subject of scientific deliberation for over a decade. For instance, simulation studies indicate that the dendrimer size increases as pH decreases from neutral to low, although the actual value of the swelling parameter depends on the applied model. Within the Debye−Hückel approximation which treats free ions implicitly the radius of gyration was shown to increase by as much as 70%,[11] whereas other approaches with explicit ions lead to a much weaker dependence of dendrimer conformations on ionic strength.[9,10,12,13] The latest, detailed molecular dynamics simulations and mean field theory[14,15] predict swelling of about 4% which is in excellent agreement with small-angle neutron scattering (SANS) measurements on PAMAMs.[5,16]

It is therefore apparent from previous studies that the degrees of freedom of counterions have to be taken into account explicitly for dendritic polyelectrolytes due to the importance of ion valence and trapping in the dendrimer volume, ion condensation and their effect on conformational changes of dendrimers.[17,18] Actually, as the strength of electrostatic interactions increases both under neutral and low pH conditions counterions penetrate not only the molecule periphery but, in the first place, its interior.[15,19−26] This leads to the reduction of the dendrimer effective charge, screening of electrostatic repulsion between charged monomers and nonmonotonous behavior of dendrimer size. Last but not least ions also play a crucial role in the formation of complexes comprised of charged dendrimers and linear polyanions and in self-organization in solutions of charged dendrimers,[27−33] though many important aspects of complexation such as dendrimer overcharging by linear polyelectrolytes have been revealed within the Debye−Hückel


Published on Web 11/24/2010

approach as well.[34−37] Obviously, it is dendrimer−DNA binding[38−48] in the first place, which being of immense interest in biosciences inspires theoretical investigations.

In this paper, we continue our coarse-grained simulation study on the effect of spacer length variation on charged dendrimers and investigate the interplay between charge effects and spacer-length scaling using the bond fluctuation model as the most effective simulation tool to explore universal properties of flexible polymers.[26,49] In this work we focus on the pH-dependence of the properties of weak dendritic polyelectrolytes such as PAMAM. Following the experimental observation we implement the most relevant cases: neutral pH-values correspond to charaging of terminal groups only, while at low pH (about 4 for the case of PAMAM) all branching points and terminal groups are charged.

The remaining part of the paper is organized as follows. In section II, we outline the model and the simulation method. The results of our simulations are presented and discussed in section III. Finally, our conclusions and remarks are given in section IV.

## II. Model and Simulations

As in our previous work, we use the bond fluctuation method (BFM) on a cubic lattice.[50,51] Details of the implementation for dendrimers can be found in our previous works[26,49]

We are simulating single dendrimers and explicit counterions in a cubic box of size $L^3 = 500 \times 500 \times 500u^3$ (where $u$ is the lattice unit) with periodic boundary conditions in all three dimensions. The molecules are modeled as a treelike macromolecular skeleton. An $2D$ schematic representation of dendrimers at low and neutral pH is shown in Figure 1.

Dendrimers of generation $G = 5$, spacer length $S = 1, 2, 4, 8$ and branching functionality $f = 3$ are generated by a divergent growth process in the ascending order of the internal generation number $0 \le g \le G$ starting from the core of two bonded monomers. The number of monomers is given by

$$N = 2 + 4S(2^G - 1) \tag{2.1}$$

The number of branching points including the terminal groups is

$$N_b = 2^{G+2} - 2 \tag{2.2}$$

and the number of terminal groups is given by

$$N_t = 2^{G+1} \tag{2.3}$$

Branching and terminal groups can carry positive charges of valence $z = 1$. For each charged group, one counterion is introduced to the simulation box, which bears a negative charge $z = -1$.

Neutral pH is simulated by charging the terminal groups only. This results in $N_t$ counterions. Low pH is simulated by charging terminal groups and all branching points. Thus, we have to add $N_b$ counterions to the system.

The electrostatic interaction between the charges is the total Coulomb energy defined as

$$E(r_{ij}) = \frac{E_c(r_{ij})}{\delta} = \frac{z_i z_j}{r_{ij}} \tag{2.4}$$

where $r_{ij}$ is the distance between the $i$th and $j$th ions with valences $z_i$ and $z_j$. The energy unit is defined as

$$\delta = \frac{e^2}{\varepsilon u} \tag{2.5}$$

with $e$ standing for the electric charge and $\varepsilon$ for the permittivity of the solvent. The long-range nature of the Coulomb interactions is treated by the Ewald summation method with the minimum image convention for the real-space term, $\kappa = 5/L$, $k_{max} = 6$ for the sum in the reciprocal space and for a conducting external medium, see.[26,52,53] We calculate thermodynamic averages at the reduced temperature $\tau = k_B T/\delta$, where $T$ is the absolute temperature and $k_B$ is the Boltzmann constant. The model can be converted to real units by the inverse relation

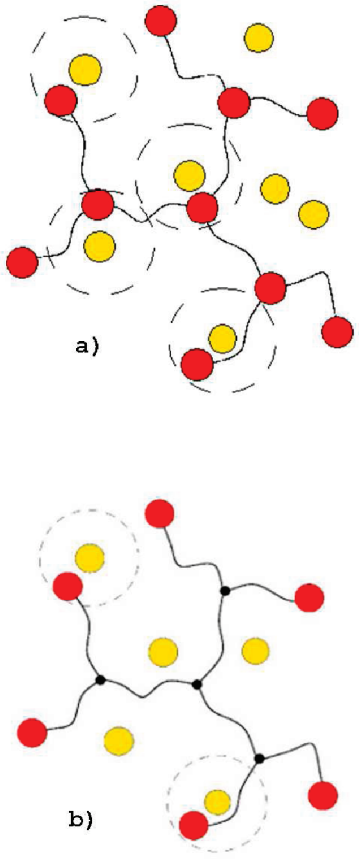


**Figure 1.** Schematic 2D picture of dendrimers under low (a) and neutral (b) pH conditions. The charged monomers (counterions) are shown with the red (yellow) spheres. Condensed counterions are indicated by dashed circles.

$$\tau = \frac{u}{\lambda_B} \tag{2.6}$$

between $\tau$ and the Bjerrum length

$$\lambda_B = \frac{e^2}{\varepsilon k_B T} \tag{2.7}$$

Within the BFM for instance, the choice of $u \approx 2$ Å corresponds to a bond length $a \approx 5$ Å, which in turn, concurs reasonably with real dendrimers.[54] In water at room temperature, one obtains $\lambda_B \approx 7$ Å and eq 2.6 yields $\tau \approx 0.3$.

Configurations are sampled using the bond fluctuation model including the standard Metropolis method.[26] In our studies, the systems were equilibrated for a maximum of $10^7$ MCS (Monte Carlo steps). One MCS consists of $N$ random selections of monomers to be moved in a randomly chosen, one of the six directions by a single lattice unit strictly ensuring excluded volume and bond constraints. Averages were calculated for $10^3$−$10^4$ equilibrium configurations stored every $10^3$th MCS.

## III. Results

**A. Counterion Condensation.** In this section, following Manning's idea developed for infinite cylindrical polyelectrolytes,[55−58] we focus on low temperature condensation of counterions on charged dendrimers.

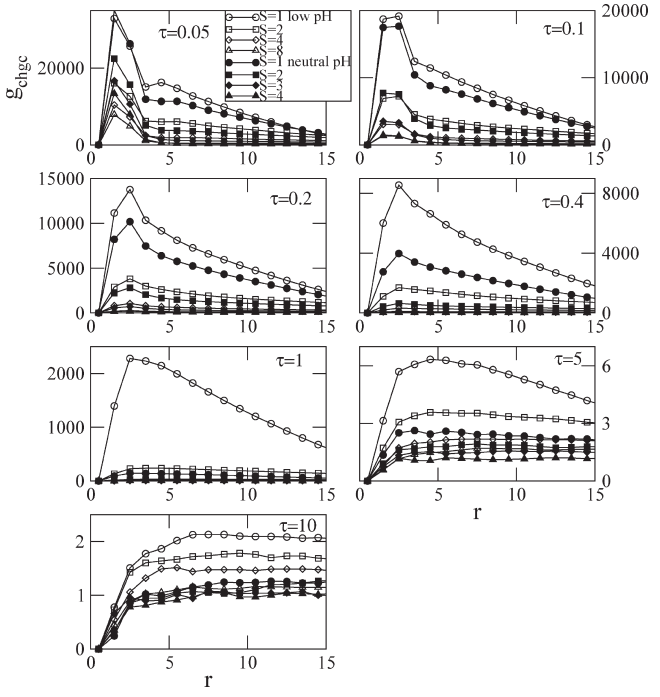


**Figure 2.** Pair correlation functions between charged groups and counterions for $G = 5$ at various temperatures and spacer lengths. The open symbols correspond to low pH-values, while the filled ones represent neutral pH.

The tendency of counterions to concentrate around the charged groups in our simulated systems can be analyzed using the pair correlation function between charged groups and counterions, $g_{chgc}$. The results are displayed in Figure 2. Sharp peaks in $g_{chgc}$ correspond to pronounced ion condensation. The disappearance of the peak at higher temperatures signals delocalization of counterions. Generally, counterion condensation is more significant for shorter spacers. The effect of pH is more pronounced at higher temperatures. In particular for $\tau = 1$ and $S = 1$ condensation can be observed for low pH, but not for neutral pH.

In order to quantify the amount of condensed counterions we adapt the simplest criterion for condensation based on the distance between ions and charged beads. In the following we assume that an ion is condensed when its distance from at least one charged unit is less than $\sqrt{6}$, a distance comparable with the average bond length in the BFM. This approach is widely used in studies on polyelectrolyte systems and has proved reasonable both for lattice and off-lattice simulations.[20−23,59] A comparison of various methods has been given by Grass and Holm.[59] We note that the peak-position of the correlation functions in Figure 2 is nearly constant. A fact which confirms this approach. In Figure 3 we plot the normalized fraction $f_c = \langle N_c \rangle / N_b$ ($f_c = \langle N_c \rangle / N_t$) of condensed counterions as a function of $\tau$, where $\langle N_c \rangle$ denotes the mean absolute number of condensed counterions. It is seen that $f_c$ increases monotonically with decreasing $\tau$ from nearly zero in the high temperature limit to some finite values in the other extreme, which in turn proves that the phenomenon of condensation takes place. We note that using the Bjerrum length, $\lambda_B = u/\tau$, for the cutoff would sharpen the decay of $f_c(\tau)$ in Figure 3. In this case and at low temperatures practically all counterions will be condensed.

At the lowest $\tau = 0.05$ nearly 90% of counterions are condensed for $S = 1$, whereas it is about 50% for $S = 8$, which reflects a general tendency that ions are more loosely tied to the charged units of dendrimers with longer spacers.

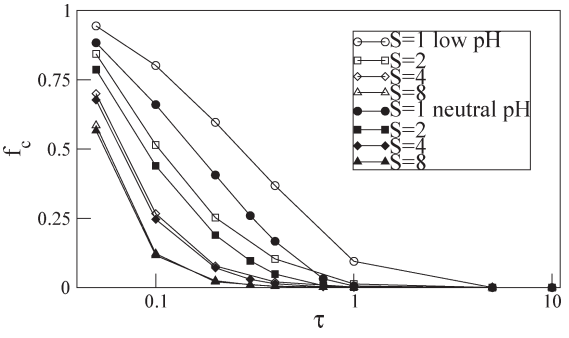


**Figure 3.** Fraction $f_c$ of condensed counterions versus $\tau$. The open (filled) symbols correspond to the dendrimer under low (neutral) pH conditions.

As indicated by Figure 3 a decrease in pH leads to some increase in $f_c$. For small spacers this effect is most pronounced. For longer spacer lengths, the influence of pH on condensation is rather minor.

We conclude that lowering pH increases counterion condensation effects, which are well pronounced at low temperature for short spacer length. For longer spacers, the effect of pH on condenstion becomes marginal.

**B. Electrostatic and pH-Driven Swelling.** In principle, the radius of gyration $R_g$ can be experimentally obtained using scattering techniques.[60−65] Although, it seems to be rather difficult, in particular for charged systems, to obtain exact values of $R_g$, some authors[5,16] report a weak change in dendrimers' size under variation of pH. The presence of electrostatic interactions and the related trapping of counterions inside the molecule tends to swell the denderimer's size. This can be analyzed directly by calculating the mean square radius of gyration:

$$\langle R_g{}^2 \rangle = \left\langle \frac{1}{N} \sum_{i=1}^{N} (r_i - r_{cm})^2 \right\rangle \tag{3.8}$$

where $r_i$ and $r_{cm}$ denote the position vectors of the $i$th monomer and of the center of mass (c.m.) of the dendrimer, respectively. In the following we use the short-hand notation $R_g = \langle R_g{}^2 \rangle^{1/2}$. For neutral dendrimers the mean-field approximation of excluded volume effects lead to spacer length scaling as we have shown in our previous work.[49] In particular, we can write

$$R_{g0}/S^{\nu} \sim (nG^2)^{1/5} \tag{3.9}$$

where $\nu = {}^3/_5$ denotes the Flory exponent and $n = N/S$ is the number of spacer chains. The index "0" denotes the uncharged state which corresponds either to very high temperatures or high salt concentrations in the experiment. When spacer scaling is valid, the extension of spacers $R_S \sim S^{\nu}$ and their self-density $S/R_S{}^3 \sim S^{1-3\nu}$ set the characteristic length scale and monomer density for dendrimers. In ref 49, we have found a very good agreement of spacer length scaling with the results for $R_{g0}$ as well as for the density profiles. Moreover, we have explicitly shown the independence of the average extension of spacers of the dendrimer generation number.

In Figure 4a, we show the rescaled radius of gyration $R_g/R_{g0}$ as a function of $\tau$ for low and neutral pH-values. In both cases $R_g$ displays a nonmonotonous behavior with respect to $\tau$, becoming comparable to $R_{g0}$ in the limit of high and low temperatures. Decreasing pH, increases swelling and the location of the swelling maximum shifts slightly toward higher values of the temperature. The maximum volume swelling, $Q = (R_g/R_{g0})^3$, observed in our simulations

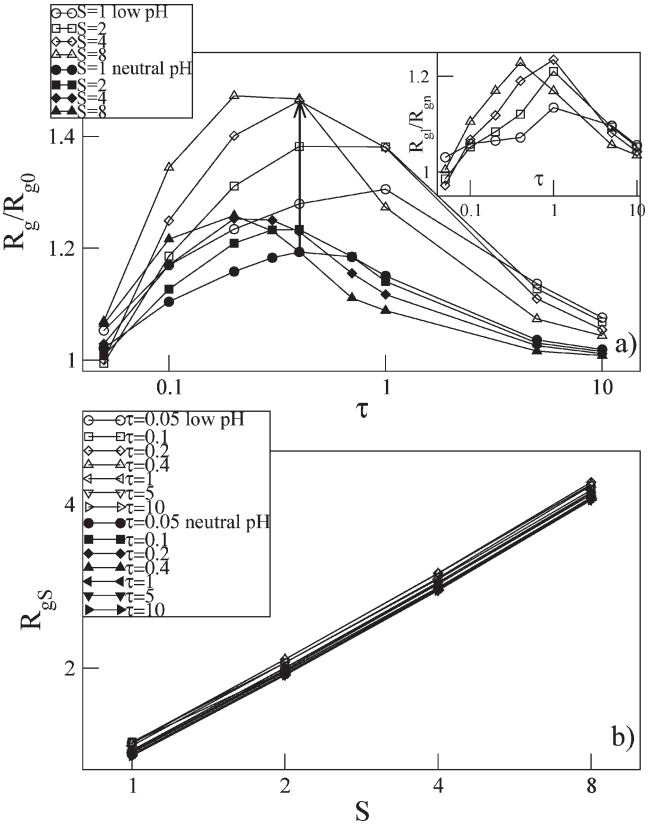


**Figure 4.** (a) Aspect ratio $R_g/R_{g0}$ between the radius of gyration of charged and neutral dendrimers versus $\tau$. The arrow indicates the pH-driven maximum swelling for long spacer molecules. The inset shows the aspect ratio $R_{gl}/R_{gn}$ between the radius of gyration of dendrimers at low and neutral pH versus $\tau$, respectively. (b) Mean radius of gyration of spacers $R_{gS}$ versus spacer length $S$ at the considered $\tau$. The open (filled) symbols correspond to the dendrimer under low (neutral) pH conditions.

corresponds to the case of the longest spacers and low pH where we obtain $Q = 3.2$. The maximum value at neutral pH corresponds to $Q = 2$.

We can define the pH-driven swelling ratio $r_{pH} = R_{gl}/R_{gn}$, where the indices "$l$" and "$n$" denote low and neutral pH, respectively. The results are displayed in the inset in Figure 4a. Our simulations clearly show that the pH-driven swelling ratio of dendrimers reveals some dependence on $S$ and $\tau$. The maximum of $r_{pH} = 1.25$ occurs for long spacers as indicated in the inset of Figure 4a and by the arrow inside the plot. Thus, pH-variation can almost double the characteristic volume of the dendrimer under good solvent conditions.

The electrostatic swelling observed in our simulations is larger than that obtained in experiments.[5,16] We note, however, that our simulations are performed in the absence of salt. Higher salt concentrations such as physiological conditions can diminish this effect considerably.

For low values of the pH the deviations between the curves for various spacer-lengths in Figure 4a are essential. At neutral pH spacer length scaling can be assumed at least approximately, see ref 26, since the deviations of the curves in Figure 4a are on the order of 10% only. In Figure 4 b) we plot the radius of gyration of spacers as a function of spacer length at various temperatures. Spacer size is nearly independent of $\tau$ but varies slightly with pH-value, a weak stretching of the spacer chains at low pH can be observed. This cannot explain the swelling behavior displayed in Figure 4 a). Thus, in general the swelling of the dendrimers due to excluded volume and charge effects is due to "unfolding" of the dendrimer and not due to stretching of spacers.

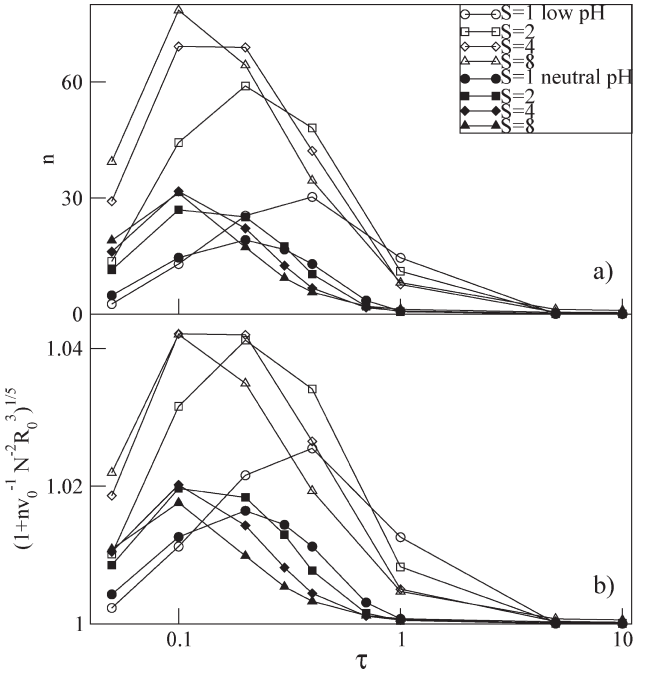


**Figure 5.** (a) Number of residual counterions vs the dimensionless temperature $\tau$. (b) Swelling behavior of the dendrimer as predicted by the mean field theory assuming counterion residual pressure as driving force. The rhs of eq 3.11 is displayed vs $\tau$.

Our simulatons clearly show that the swelling compliance of the dendrimers is increased due to the presence of flexible spacers. This concerns in particular the response to changes in pH.

In order to understand the interplay between excluded volume effects and charges we extent an approach which was proposed earlier by Giupponi, Buzza, and Adolf.[15] Following ref 15, we consider first the swelling effect caused by the confinement of counterions which are neither condensed nor far outside the dendimer's volume. Let us call theses counterions "residual counterions" and denote their number by $n$. More precisely, $n$ is the number of residual counterions trapped within a distance $2R_g$ from the center of mass of the dendrimer. Our choice of the trapping distance is based on the observation that the radial counterion density practically drops to zero at $r/R_g \approx 2$; see Figure 10. The number of residual counterions as a function of $\tau$ is plotted explicitly in Figure 5a. The osmotic pressure exerted by the residual counterions is approximated by an ideal gas law. The generalized Flory-type free energy per dendrimer with an extension $R$ is given by

$$\frac{F}{kT} = \frac{N}{(GS)^2}R^2 + \frac{v_0 N^2}{R^3} + n\ln\left(\frac{3n}{4\pi R^3}\right) \qquad (3.10)$$

The first term corresponds to the Gaussian elasticity of treads (paths from the core to the terminal groups) and the second term denotes the mean excluded volume interaction, where $v_0$ is the excluded volume parameter. We have chosen dimensionless units with the segment length set to unity. The third term corresponds to the free energy of an ideal gas of the residual counterions. Without the effect of counterions minimization of the free energy leads to the result for neutral dendrimers, $R_{g0}$, and to spacer scaling as has been shown in ref.[49] Including the counterion pressure the minimization problem for the free energy with respect to $R$ leads to a polynomial equation of order five. Since we know that the swelling due to counterions is a rather small effect, see

Figure 4a, we apply a first order perturbation approximation which leads to the following result

$$\frac{R_g}{R_{g0}} = \left(1+\frac{nR_{g0}^3}{v_0N^2}\right)^{1/5} = (1+\Delta_{CI})^{1/5} \qquad (3.11)$$

where $R_{g0}$ denotes the extension of the corresponding neutral dendrimer. Here, we have defined the contribution of the residual counterions to swelling by $\Delta_{CI}$. The dependence on $\tau$ and pH is expressed by the number of residual counterions, $n$. We note that spacer-length scaling is broken in this result. First, ${R_0}^3/N^2$ does not depend on the number of spacers only, but scales as $S^{-1/5}$. Second, also $n$ depends on $S$, see Figure 5a, and this actually dominates the overall behavior.

In Figure 5b, we display the result of the rhs of eq 3.11 with a value of $v_0$ read off for neutral molecules we have studied before.[49] The plots show qualitative similarities with the behavior of $R_g/R_{g0}$ given in Figure 4a. Clearly, the nonmonotonous swelling behavior as a function of temperature is also displayed for the residual counterions and also the impact of spacer length. Moreover, the pH dependence qualitatively agrees. However, the absolute amount of swelling is underestimated.

Another source of swelling are counterions which escape the gyration volume of the dendrimer and thus lead to a residual, uncompensated charge inside the dendrimer. Let us denote the number of "evaporated" counterions (which is equal to the number of residual charges) by $m$. For simplicity we assume an electrostatic energy of the dendrimer corresponding to a homogeneously charged sphere given by

$$E/k_BT = \frac{3}{20\pi}m^2\frac{\lambda_B}{R} \qquad (3.12)$$

The unscreened electrostatic interaction then leads to a generalization of eq 3.10 according to

$$\frac{F}{kT} = \frac{N}{(GS)^2}R^2 + \frac{v_0N^2}{R^3} + n\ln\left(\frac{3n}{4\pi R^3}\right) + \frac{3m^2\lambda_B}{20\pi R} \qquad (3.13)$$

The generalized result for the swelling of the dendrimer in a first order approximation is then given by

$$\frac{R_g}{R_{g0}} = (1+\Delta_{CI}+\Delta_{RC})^{1/5} \qquad (3.14)$$

with

$$\Delta_{RC} = \frac{m^2{R_{g0}}^2}{20\pi N^2 v_0\tau} \qquad (3.15)$$

where we have used eq 2.6. In Figure 6a, we have plotted the total number of residual charges, $m$. It displays a monotonous increase with increasing temperature. Clearly, in the limit of very high temperature, all counterions are delocalized and the residual charge is equal to the total charge of the dendrimer. In Figure 6b, we show the direct contribution of the residual charges to the swelling behavior in the absence of counterion pressure. By comparing with Figure 5b, we see that electrostatic repulsion of residual charges is the smaller contribution, but becomes important at higher temperatures. Note that residual charges have a stronger impact for smaller spacer-length. In Figure 6c, we display the total contribution of residual counterions and charges to swelling. The effect of residual charges slightly increases the swelling at higher temperatures.

Although the swelling predicted by the Flory-type argument remains much lower as compared to the simulation

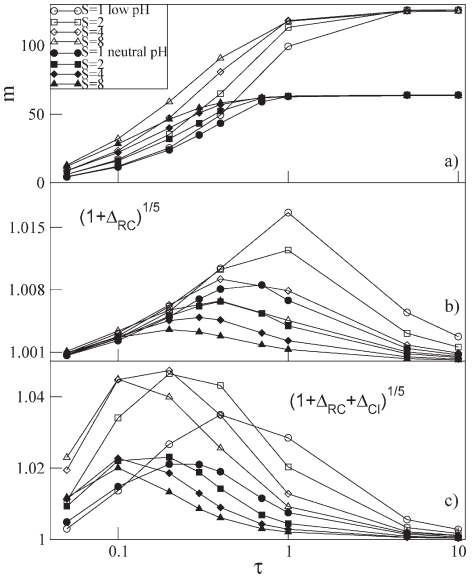


**Figure 6.** Residual charge and its contribution to the electrostatic swelling of the dendrimer as a function of temperature. (a) Number of residual charges, $m$. (b) Contribution of the residual charges to swelling. (c) Total contribution of the residual counterions and residual charges to swelling.

results in Figure 4a, the curves display many common features. In detail, we observe a significant shift of the swelling maximum with spacer length. Increasing the spacer length shifts the maximum to lower values of temperature and increases its absolute value. This effect is most pronounced for low pH. However, at higher temperatures (right to the maximum) the swelling dependence on spacer length is inverted: dendrimers with smaller spacers show a slightly higher degree of swelling. The last result can be directly interpreted by the effect of residual charges, which becomes important at higher temperatures. We note that these details are perfectly reflected by the Flory result given in Figure 6c.

Quantitative agreement between swelling and the Flory-type approach cannot be established. Apparently, the swelling predicted by the Flory-argument is much weaker than directly observed. A possible reason for the failure of the Flory-type argument is the well-known overestimation of both the (Gaussian) elasticity (entropy reduction due to swelling) and the mean-field excluded volume interactions.[66] While in combination both effects might cancel to a certain amount and lead to satisfying agreement with the simulation data, additional contributions (such as counterion pressure and electrostatic interactions) which are rather correctly treated in their absolute value are, therefore, relatively underestimated. This might explain the much weaker swelling effect predicted by the Flory approach in contrast to the agreement with many other details such as the effects of pH, temperature and spacer length, compare Figures 4a and 6c, as well as the location of the maxima of the swelling curves. To correct for this effect, one might introduce a numerical prefactor which enhances the additional contributions to an equal amount. In fact, using a prefactor of about 20 for the residual counterion and for the residual charge good quantitative agreement between the Flory model and the simulated swelling behavior can be obtained, see Figure 7. Here, we display the ratio between the rescaled result of eqs 3.14 and the directly observed swelling ratio. We note here that this states a general problem when using a Flory-type argument involving additional components for the free energy. Finite extensibility of

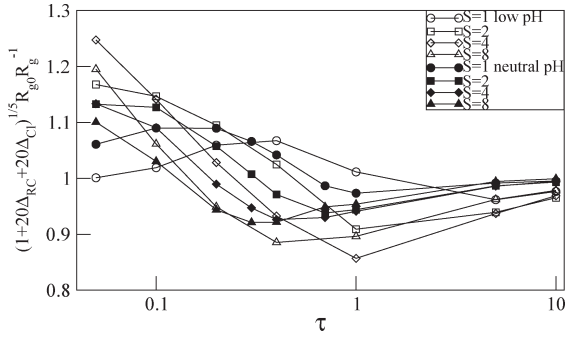


**Figure 7.** Ratio between the rhs of eq 3.14 with the prefactor of 20 for the residual counterion and for the residual charge and the aspect ratio $R_g/R_{g0}$ plotted in Figure 4a.

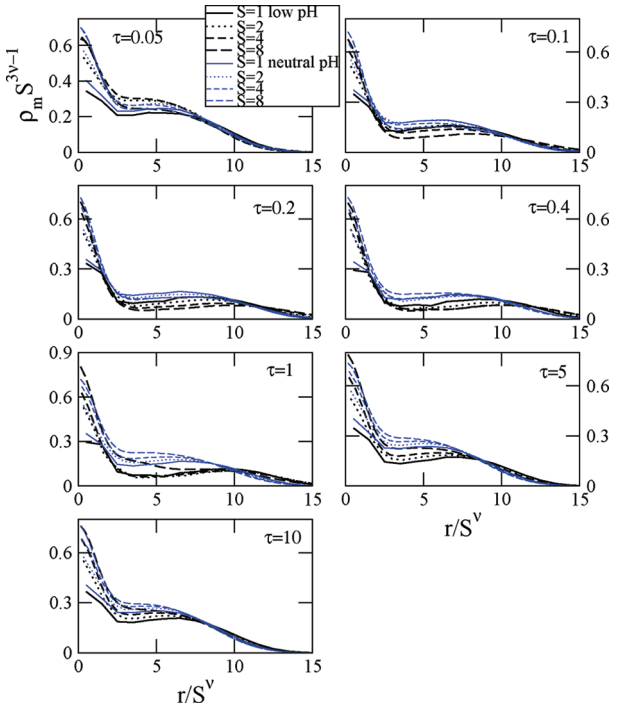


**Figure 8.** Rescaled radial monomer density $\rho_m$ versus the rescaled distance from the dendrimers' c.m. at various $\tau$. The black (blue) lines correspond to the dendrimer under low (neutral) pH conditions.

spacer chains should be less important because of the rather weak extension of spacer chains, see Figure 4b, under the conditions of our simulations. Taking into account higher order virial coefficient would even increase the conformational part of the free energy.[67]

**C. Spatial Distribution of Monomers and Terminal Groups.** We analyze the spatial distribution of monomers in terms of the self-density of spacers. In Figure 8, we show the radial monomer density profiles $\rho_m$ as functions of the distance from the dendrimers' c.m. at the considered reduced temperatures $\tau$.

Generally, our simulations[26,49] confirm the so-called dense core picture of charged dendrimers both under low and neutral pH conditions as well as for neutral dendrimers. No matter the solution pH there is a high concentration of monomers close to the c.m. that corresponds to the dense core of the molecules. At larger distances the monomer density drops sharply down to a local minimum followed by a broad maximum/plateau within the actual dendritic domain. Finally, on the periphery $\rho_m$ goes down to zero.

In our previous work we have found excellent agreement with spacer length scaling for neutral dendrimers[49] and

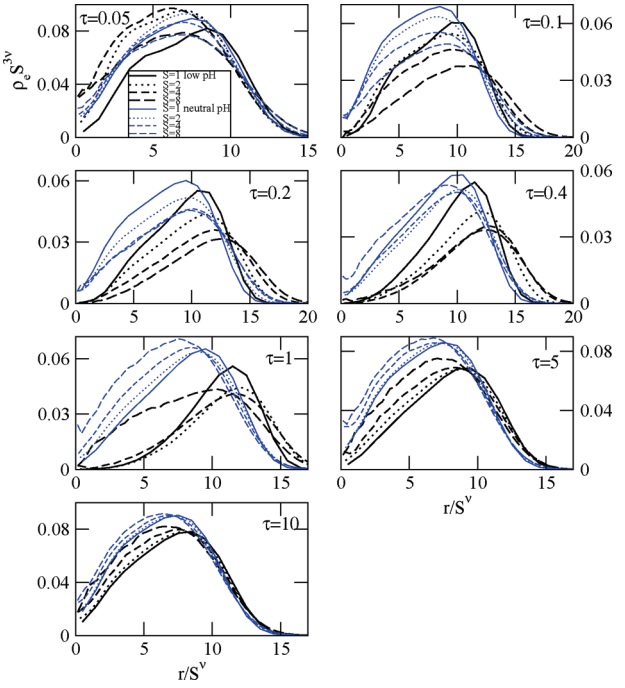


**Figure 9.** Rescaled radial density of terminal groups $\rho_e$ versus the rescaled distance from the dendrimers' c.m. at various $\tau$. The black (blue) lines correspond to the dendrimer under low (neutral) pH conditions.

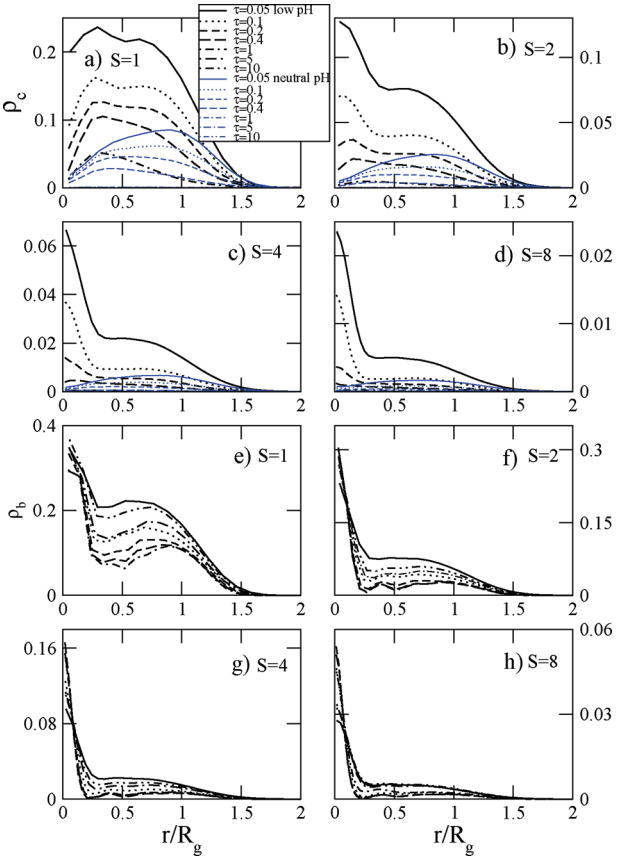


**Figure 10.** Radial counterion density $\rho_c$ (a−d) and overall radial density $\rho_b$ of branching groups (e−h) versus the rescaled distance from the dendrimers' c.m. at various $\tau$. The black (blue) lines correspond to the dendrimer under low (neutral) pH conditions.

reasonable agreement for terminally charged dendrimers (neutral pH).[26] From this we have concluded that charging

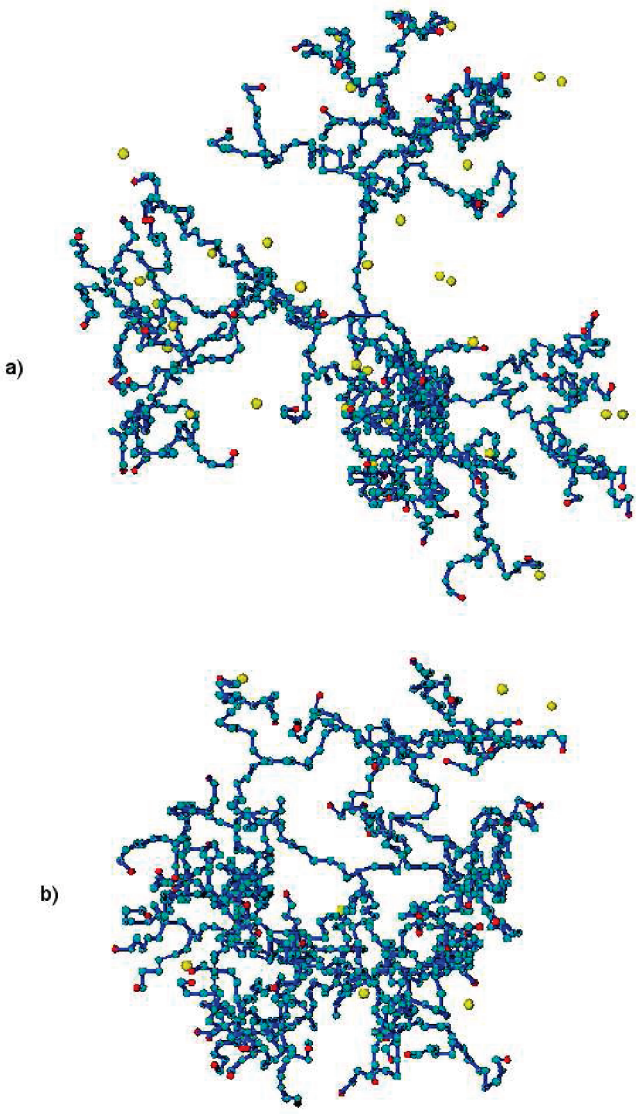


**Figure 11.** Snapshots of dendrimer/counterions configurations at (a) low and (b) neutral pH-values for $S = 8$, $\tau = 0.4$. The terminal groups (counterions) are shown with red (yellow) spheres.

might be considered as a weak force that leads only to a perturbation of the properties of neutral dendrimers which are still dominated by excluded volume effects. As can be observed from Figure 8, this is somewhat changed at low pH values. In particular, at the temperatures $\tau = 1$ and $\tau = 5$ rather large deviations between the two pH-states can be found. Although there are some deviations in spacer-length scaling we have to note that there is essentially a collapse of data. This concurs with the observation of nearly constant extension of spacers, see Figure 4. Thus, also at low pH-values swelling takes place by "unfolding" of the molecule.

In Figure 9 we show the scaled radial density of terminal groups $\rho_e$ as a function of the rescaled distance. Spacer-length scaling can be observed at very low and very high temperature, where the dendrimer behaves nearly as neutral, see Figure 4. Substantial difference between the profiles for different pH conditions can be again observed between $\tau = 0.4$ and $\tau = 1$. In particular, for the shortest spacer length one observes a pronounced peak of the distribution at low pH which indicates a localization of terminal groups at the dendrimers periphery. In this temperature range the distribution of terminal groups depends sensitively on pH. Lowering

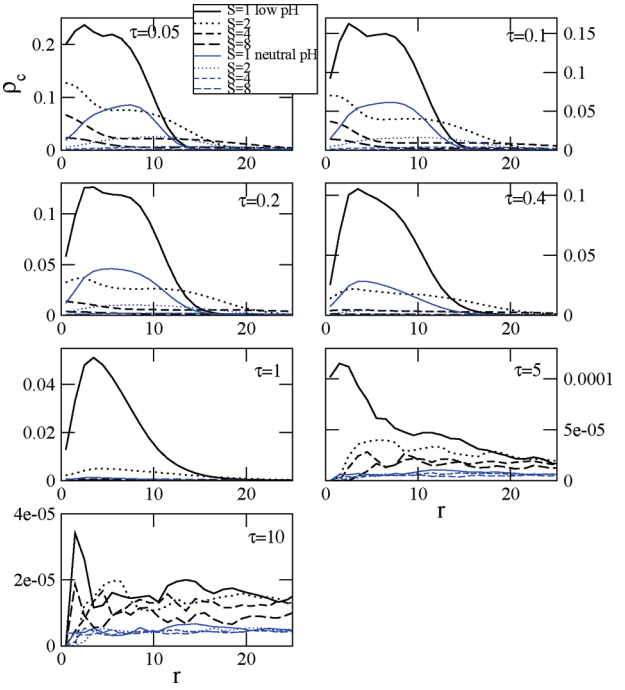


**Figure 12.** Radial counterion density $\rho_c$ versus the distance from the dendrimers' c.m. at various $S$. The black (blue) lines correspond to the dendrimer under low (neutral) pH conditions.

the pH-value swells the molecules and the terminal groups concentrate on the periphery. We have also evaluated the structure factor of the monomers. However, the effects of pH are rather weak here and the reader is therfore referred to our previous work.[26]

**D. Spatial Distribution of Counterions.** In Figure 10a−d we display the counterion radial density $\rho_c$ plotted versus the rescaled radial distance $r/R_g$ from the dendrimer's c.m. for low and neutral pH-values. It is seen that in both cases ion trapping in the dendrimer volume occurs. Since the absolute number of counterions at neutral pH is smaller so is their counterion density in the area of interest at given $\tau$ and $S$.

Interestingly, the counterion profiles are significantly different in shape. At neutral pH they are bell-shaped with a broad maximum well in the domain. At low pH the maximum is shifted toward the vicinity of the core where at lower temperatures and longer spacers it even peaks. We note that ion distribution at low pH follows closely the distribution of branching units $\rho_b$, see Figure 10e−h. On the other hand, for neutral pH, the ion distribution follows the distribution of terminal groups. Thus, the ion distribution follows mainly the distribution of the charged groups.

Counterions are well localized in the space occupied by the dendrimer at lower temperatures. This tendency weakens as $\tau$ increases and, in the extreme of high $\tau$, ions evaporate from the dendrimer and are distributed all over the space, see also snapshots in Figure 11. Note that, as presented in Figure 12, due to greater dendrimer volume for longer spacers, $\rho_c$ is reduced substantially at given $\tau$.

A quantitative measure of counterion trapping in the dendrimer's volume is the normalized fraction $f_t$ of counterions located at the distance less than $2R_g$ from the dendrimer's center of mass. As shown in Figure 13a for both pH conditions $f_t$ drops from around one down to nearly zero with increasing $\tau$. Thus, our calculations indicate that at the lowest temperature practically all counterions are localized around the dendrimer center of mass within a sphere of radius $2R_g$. The pH effect on trapping counterions inside the

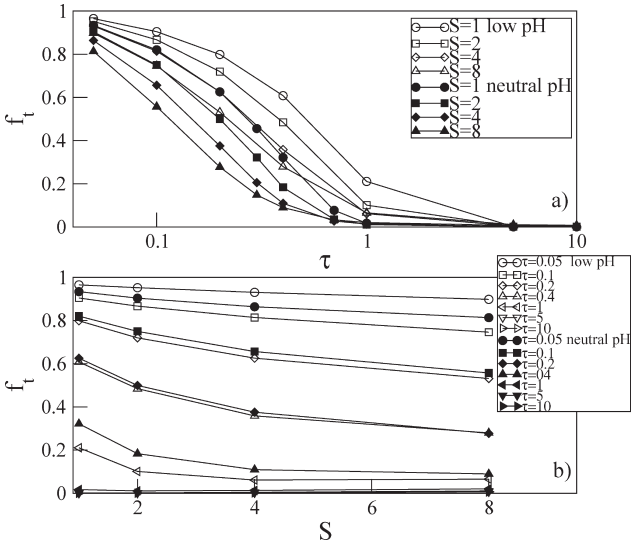


**Figure 13.** (a) Mean fraction of counterions $f_t$ located at the distance less than $2R_g$ from the dendrimer's c.m. versus $\tau$. (b) mean fraction of counterions $f_t$ located at the distance less than $2R_g$ from the dendrimer's c.m. versus $S$ at fixed $\tau$. The open (filled) symbols correspond to the dendrimer under low (neutral) pH conditions.

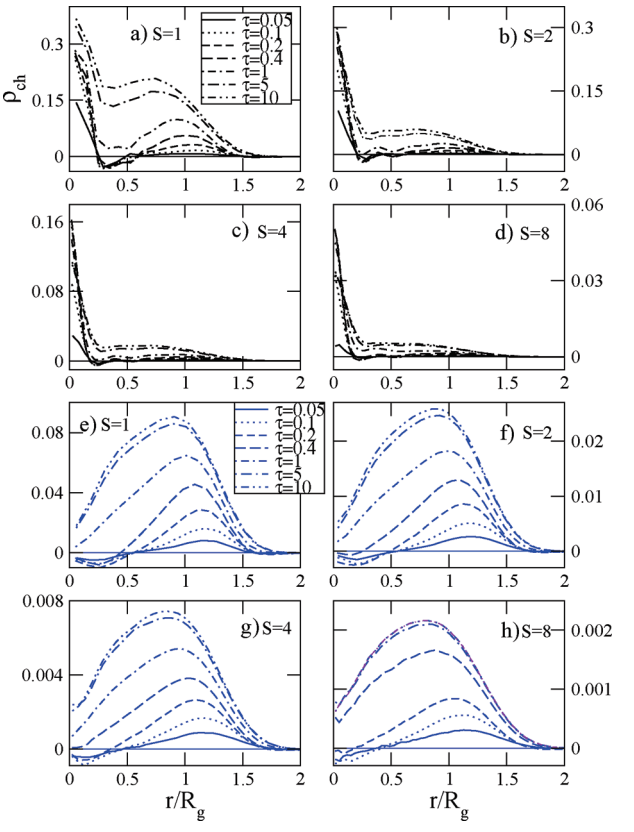


**Figure 14.** Overall charge density $\rho_{ch}$ versus the rescaled distance from the dendrimers' c.m. $r/R_g$ at various $\tau$. The black (blue) lines correspond to the dendrimer under low (neutral) pH conditions. The horizontal lines refer to $\rho_{ch} = 0$.

molecule is relatively weak. Although there is a tendency to increase the trapping with lowering pH the effect of temperature is dominating as can be seen in Figure 13b. There is only a weak effect of spacer length on the counterion trapping.

The mean overall charge density $\rho_{ch} = \rho_b - \rho_c$ ($\rho_{ch} = \rho_e - \rho_c$) obtained for dendrimers under low and neutral pH conditions is shown in Figure 14. Generally speaking at sufficiently high temperatures the shape of $\rho_{ch}$ follows that of the overall density of the corresponding dendrimer groups bearing charges, i.e., either the branching groups or terminal ones, see Figures 9 and 10. However, with lowering temperature the counterion density $\rho_c$ in the dendrimer domain increases and the overal charge density $\rho_{ch}$ reveals some tendency to change its sign in the vicinity of the core. For the charged branching points this is particularly the case for $S = 1$ for which $\rho_{ch}$ is first positive in the core, decreases sharply to a shallow, negative minimum and subsequently takes small but positive values again. On the other hand, for terminally charged dendrimers $\rho_{ch}$ is negative in the core and subsequently becomes positive further from it.

## IV. Conclusions

We have used the bond fluctuation model to investigate the effect of pH for weak dendritic polyelectrolytes with flexible spacers and explicit counterions over a wide range of reduced temperatures. Our model has been chosen to mimic such molecules as PAMAMs which become positively charged around pH 7 due to protonation of the terminal primary amines and whose charge further increases by protonation of the tertiary amines in the branching groups at pH-values below 5.

Charging of the dendrimer leads to swelling. The degree of swelling, which can be characterized by the change of the radius of gyration with respect to the uncharged state depends non-monotonously on temperature displaying a pronounced maximum. The maximum volume degree of swelling of dendritic polyelectrolytes increases when pH is dropped from 7 to below 5.

In order to understand the swelling effect we have considered two driving forces: The osmotic pressure of noncondensed counterions which are trapped within the dendrimer's volume and which we call residual counterions. Uncompensated charges of the dendrimer which result from evaporation of counterions into the solution give rise to long-range electrostatic repulsion.

We have used a Flory-type argument to quantify the contribution of the two swelling forces. Given the fact that the swelling is rather low, we applied a first order approximation to solve the nonlinear equation for the swelling equilibrium. This model displays the main aspects of the swelling behavior such as the dependence on temperature, pH and spacer length. However, quantitatively the electrostatic swelling effect is underestimated when using the excluded volume constant calculated from the data for the uncharged dendrimer (which displays very good agreement with the Flory-type prediction and corresponding spacer-length scaling). A possible origin for the discrepancy can be the well-known overestimation of Gaussian elasticity and mean-field excluded volume interaction. Other contributions to the Free Energy, which are quantitatively more accurate are thus relatively underestimated. Scaling-up counterion and electrostatic contributions by a factor of about 20 we obtain good quantitative results for the swelling effect. However, we note that even with free fitting parameters for both contributions a perfect agreement between the Flory-type prediction and the simulated data cannot be achieved.

Decreasing the pH-value leads to (higher) swelling of the dendrimer with a shift in the swelling-maximum toward higher temperatures. The effect is most pronounced for long spacers where the volume swelling is increased up to a factor of almost 2 when lowering the pH-value. The swelling due to protonation is due to unfolding of the dendrimer, and the terminal groups tend to concentrate on the periphery.

It should be pointed out that our results are presented as functions of the reduced temperature (inverse Bjerrum length) and not of the absolute temperature. Therefore, by definition,

variations in the former can be experimentally realized by variations either in the absolute temperature or in the dielectric permittivity of the solvent. Changes in one of these parameters in experiments would affect the actual value of the reduced temperature and the properties of the dendrimers accordingly. We note that the nonmonotonous behavior of dendrimers' swelling with respect to the reduced temperature is similar to that of charged polymer brushes.[68] Also in this case noncondensed but trapped counterions exert an osmotic pressure which swells the brush.

To conclude, long, flexible spacers lead to increased volume response of dendritic weak polyelectrolytes with respect to changes in pH. The interplay between pH, spacer length and temperature can be applied to systhesize tailor-made dendrimers which display optimal pH-controlled swelling/shrinking effects in a desired temperature range.

**Acknowledgment.** Support from the Deutsche Forschungsgemeinschaft (DFG) Contract No. SO-277/2-1 is gratefully acknowledged. Part of the calculations were carried out at the Center for High Performance Computing (ZIH) of the TU Dresden.

## References and Notes

(1) DeLong, R.; Stephenson, K.; Loftus, T.; Fisher, M.; Alahari, S.; Nolting, A.; Juliano, R. L. *J. Pharm. Sci.* **1997**, *86*, 762.
(2) Yoo, H.; Sazani, P.; Juliano, R. L. *Pharm. Res.* **1999**, *16*, 1799.
(3) Kukowska-Latallo, J. F.; Bielinska, A.; Johnson, J.; Spindler, R.; Tomalia, D. A.; Baker, J. R. *Proc. Natl. Acad. Sci.* **1996**, *93*, 4897.
(4) Khan, M. K.; Nigavekar, S. S.; Minc, L. D.; Kariapper, M. S. T.; Nair, B. M.; Lesniak, W. G.; Balogh, L. P. *Technol. Cancer Res. Treat*. **2005**, *4*, 603.
(5) Nisato, G.; Ivkov, R.; Amis, E. J. *Macromolecules* **2000**, *33*, 4172.
(6) van Duijvenbode, R. C.; Borkovec, M.; Koper, G. J. M. *Polymer* **1998**, *39*, 2657.
(7) Kabanov, V. A.; Zezin, A. B.; Rogacheva, V. B.; Gulyaeva, Z. G.; Zansochova, M. F.; Joosten, J. G. H.; Brackman, J. *Macromolecules* **1998**, *31*, 5142.
(8) Paulo, P. M. R.; Lopes, J. N. C.; Costa, S. M. B. *J. Phys. Chem. B* **2007**, *111*, 10651.
(9) Maiti, P. K.; Çağin, T.; Lin, S.; Goddard, I. W. A. *Macromolecules* **2005**, *38*, 979.
(10) Maiti, P. K.; Goddard, I. W. A. *J. Phys. Chem. B* **2006**, *110*, 25628.
(11) Welch, P.; Muthukumar, M. *Macromolecules* **1998**, *31*, 5892.
(12) Lee, I.; Athey, B. D.; Wetzel, A. W.; Meixner, W.; Baker, J. J. R. *Macromolecules* **2002**, *35*, 4510.
(13) Opitz, A. W.; Wagner, N. J. *J. Polym. Sci., Part B: Polym. Phys.* **2006**, *44*, 3062.
(14) Liu, Y.; Bryantsev, V. S.; Diallo, M. S.; Goddard, I. W. A. *J. Am. Chem. Soc.* **2009**, *131*, 2798.
(15) Giupponi, G.; Buzza, D. M. A.; Adolf, D. B. *Macromolecules* **2007**, *40*, 5959.
(16) Chen, W.; Porcar, L.; Liu, Y.; Butler, P. D.; Magid, L. J. *Macromolecules* **2007**, *40*, 5887.
(17) Blaak, R.; Lehmann, S.; Likos, C. N. *Macromolecules* **2008**, *41*, 4452.
(18) Ballauff, M.; Likos, C. N. *Angew. Chem., Int. Ed.* **2004**, *43*, 2998.
(19) Galperin, D. E.; Ivanov, V. A.; Mazo, M. A.; Khokhlov, A. R. *Polym. Sci. Ser. A* **2005**, *47*, 61.
(20) Gurtovenko, A. A.; Lyulin, S. V.; Karttunen, M.; Vattulainen, L. *J. Chem. Phys.* **2006**, *124*, 094904.
(21) Majtyka, M.; Kłos, J. *Phys. Chem. Chem. Phys.* **2007**, *9*, 2284.
(22) Majtyka, M.; Kłos, J. *J. Phys.: Condens. Matter* **2006**, *18*, 3581.
(23) Majtyka, M.; Kłos, J. *Acta Phys. Pol., A* **2006**, *110*, 833.
(24) Lin, Y.; Liao, Q.; Jin, X. *J. Phys. Chem. B* **2007**, *111*, 5819.
(25) Tian, W.; Ma, Y. *J. Phys. Chem. B* **2009**, *113*, 13161.
(26) K9os, J. S.; Sommer, J.-U. *Macromolecules* **2010**, *43*, 4418.
(27) Tanis, I.; Karatasos, K. *Phys. Chem. Chem. Phys.* **2009**, *11*, 10017.
(28) Lyulin, S. V.; Vattulainen, I.; Gurtovenko, A. A. *Macromolecules* **2008**, *41*, 4961.
(29) Maiti, P. K.; Bagchi, B. *Nano Lett.* **2006**, *6*, 2478.
(30) Tian, W.; Ma, Y. *Macromolecules* **2010**, *43*, 1575.
(31) Karatasos, K. *Macromolecules* **2008**, *41*, 1025.
(32) Karatasos, K.; Krystallis, M. *Macromol. Symp.* **2009**, *278*, 32.
(33) Karatasos, K.; Krystallis, M. *J. Chem. Phys.* **2009**, *130*, 114903.
(34) Lyulin, S. V.; Darinskii, A. A.; Lyulin, A. V. *Macromolecules* **2005**, *38*, 3990.
(35) Lyulin, S. V.; Darinskii, A. A.; Lyulin, A. V. *Phys. Rev. E* **2008**, *78*, 041801.
(36) Larin, S.; Lyulin, S.; Lyulin, A.; Darinskii, A. *Polym. Sci., Ser. A* **2009**, *51*, 459.
(37) Lyulin, S.; Karatasos, K.; Darinskii, A.; Larin, S.; Lyulin, A. *Soft Matter* **2008**, *4*, 453.
(38) Tang, M. X.; Redemann, C. T.; Szoka, J. F. C. *Bioconjugate Chem.* **1996**, *7*, 703.
(39) Kabanov, V. A.; Zezin, A. B.; Rogacheva, V. B.; Gulyaeva, Z. G.; Zansochova, M. F.; Joosten, J. G. H.; Brackman, J. *Macromolecules* **1904**, *32*, 1999.
(40) Kabanov, V. A.; Sergeyev, V. G.; Pyshkina, O. A.; Zinchenko, A. A.; Zezin, A. B.; Joosten, J. G. H.; Brackman, J.; Yoshikawa, K. *Macromolecules* **2000**, *33*, 9587.
(41) Gössl, I.; Shu, L.; Schlüter, A. D.; Rabe, J. *J: Am. Chem. Soc.* **2002**, *124*, 6860.
(42) Shifrina, Z. B.; Kuchkina, N. V.; Rutkevich, P. N.; Vlasik, T. N.; Sushko, A. D.; Izmrudov, V. A. *Macromolecules* **2009**, *42*, 9548.
(43) Imae, T.; Miura, A. *J. Phys. Chem. B* **2003**, *107*, 8088.
(44) Mitra, A.; Imae, T. *Biomacromolecules* **2004**, *5*, 69.
(45) Leisner, D.; Imae, T. *J. Phys. Chem. B* **2004**, *108*, 1798.
(46) Örberg, M. L.; Schillen, K.; Nylander, T. *Biomacromolecules* **2007**, *8*, 1557.
(47) Ritort, F.; Mihardja, S.; Smith, S. B.; Bustamante, C. *Phys. Rev. Lett.* **2006**, *96*, 118301.
(48) Störkle, D.; Duschner, S.; Heimann, N.; Maskos, M.; Schmidt, M. *Macromolecules* **2007**, *40*, 7998.
(49) Kłos, J. S.; Sommer, J.-U. *Macromolecules* **2009**, *42*, 4878.
(50) Carmesin, I.; Kremer, K. *Macromolecules* **1988**, *21*, 2819.
(51) Trautenberg, H. L.; Hölzl, T.; Göritz, D. *Comput. Theor. Polym. Sci.* **1996**, *6*, 135.
(52) Allen, M. P.; Tildesley, D. J. *Computer Simulation of Liquids*; Clarendon Press: Oxford, U.K., 1984.
(53) Rapaport, D. C. *The Art of Molecular Dynamics Simulation*, 2nd ed.; Cambridge University Press: Cambridge, U.K., 2004.
(54) Pavlov, G. M.; Korneeva, E. V.; Meijer, E. W. *Colloid Polym. Sci.* **2002**, *280*, 416.
(55) Manning, G. S. *J. Chem. Phys.* **1969**, *51*, 924.
(56) Manning, G. S. *J. Chem. Phys.* **1969**, *51*, 934.
(57) Manning, G. S. *J. Chem. Phys.* **1969**, *51*, 3249.
(58) Manning, G. S. *J. Chem. Phys.* **1988**, *89*, 3773.
(59) Grass, K.; Holm, C. *Soft Matter* **2009**, *5*, 2079.
(60) Prosa, T. J.; Bauer, B. J.; Amis, E. J.; Tomalia, D. A.; Scherrenberg, R. *J. Polym. Sci., Part B: Polym. Phys.* **1997**, *35*, 2913.
(61) Pötschke, D.; Ballauff, M.; Lindner, P.; Fischer, M.; Vögtle, F. *Macromolecules* **1999**, *32*, 4079.
(62) Prosa, T. J.; Bauer, B. J.; Amis, E. J. *Macromolecules* **2001**, *34*, 4897.
(63) Rosenfeldt, S.; Dingenouts, N.; Ballauff, M.; Werner, N.; Vögtle, F.; Lindner, P. *Macromolecules* **2002**, *35*, 8098.
(64) Rathgeber, S.; Pakula, T.; Urban, V. *J. Chem. Phys.* **2004**, *121*, 3840.
(65) Rathgeber, S.; Monkenbusch, M.; Kreitschmann, M.; Urban, V.; Brulet, A. *J. Chem. Phys.* **2002**, *117*, 4047.
(66) P. de Gennes, *Scaling Concepts in Polymer Physics*; Cornell University Press: Ithaca, NY, and London, 1979.
(67) Lyulin, S. V.; Evers, L. J.; van der Schoot, P.; Darinskii, A. A.; Lyulin, A. V.; Michels, M. A. J. *Macromolecules* **2004**, *37*, 3049.
(68) He, S.-Z.; Merlitz, H.; Chen, L.; Sommer, J.-U.; Wu, C.-X. *Macromolecules* **2010**, *43*, 7845.